IJIREEICE ISSN (O) 2321-2004, ISSN (P) 2321-5526

International Journal of Innovative Research in Electrical, Electronics, Instrumentation and Control Engineering

Impact Factor 8.414 ⁜ Peer-reviewed & Refereed journal ⁜ Vol. 13, Issue 11, November 2025

DOI: 10.17148/IJIREEICE.2025.131119

INNOVATIVE MPPT TRACKING TECHNIQUES FOR INTEGRATED WIND AND PHOTOVOLTAIC ENERGY SYSTEMS

M. Divakar[1], U. Lakshmi[2]

PG Student, Department of Electrical Engineering, Sankethika Vidya Parishad Engineering College, Andhra pradesh, India[1]

Assistant professor, Department of Electrical Engineering, Sankethika Vidya Parishad Engineering College, Andhra Pradesh, India[2]

Abstract: Traditional techniques employed to monitor the maximum power point in wind energy conversion systems (WECS) encounter numerous challenges. One of the most prevalent methods is the perturb and observe (P&O) algorithm, which tracks and logs the highest achievable power point. Nevertheless, a significant drawback of this algorithm is the challenge of determining an optimal step size. To tackle this problem, this research introduces an innovative approach that combines fuzzy logic control with the trapezoidal rule. The suggested method is evaluated against two existing techniques: the trapezoidal rule-based P&O (TRPO) algorithm and the standard P&O method. MATLAB/Simulink simulations are conducted to assess the performance of all three algorithms under randomly fluctuating wind speeds. The findings indicate that the proposed approach markedly decreases power oscillations while improving DC output current, voltage, and power. Furthermore, this study expands the methodology by integrating a wind-solar hybrid system with an artificial neural network (ANN) model, thereby enhancing the efficiency and stability of renewable energy generation.

I. OVERVIEW

The global demand for energy has risen considerably due to swift industrial development, improved living standards, and population growth. This increase in energy usage has resulted in the exhaustion of traditional resources such as coal, gas, and oil. To tackle this challenge and foster a sustainable future, renewable energy sources have become increasingly favored for their environmental advantages and capacity to fulfill energy needs. Among these sources, wind energy is particularly notable as a clean and effective means of power generation [1]. A Wind Energy Conversion System (WECS) is specifically engineered to capture wind energy and transform it into electrical energy through the use of power conversion equipment and wind turbines (WT). Nevertheless, wind is an inherently variable resource, which complicates the efficient extraction of maximum power. The main function of a wind turbine is to seize wind energy and convert it into mechanical energy, which is subsequently converted into electrical power during the generator stage, as depicted in Figure 1.

A. Wind Turbine Generators

Various types of generators are utilized in Wind Energy Conversion Systems (WECS), each presenting its own set of advantages and disadvantages:

Squirrel Cage Induction Generator (SCIG):

Provides high reliability, low complexity, and cost-effectiveness.

Nonetheless, it necessitates external excitation and exhibits lower efficiency.

Doubly Fed Induction Generator (DFIG):

Operates efficiently with partial-scale power converters, rendering it a cost-effective option compared to SCIG.

However, it demands a multi-stage gearbox and excitation system, which adds to its complexity [2, 3, 4].

Permanent Magnet Synchronous Generator (PMSG):

Self-excited, extremely reliable, and cost-effective, making it a highly favored option [5, 6].

Table 1 presents a compilation of abbreviations and nomenclature employed in this research.

B. Maximum Power Point Tracking (MPPT) in WECS

Due to fluctuations in wind speed, the power output of a wind turbine varies. To enhance power extraction in changing wind conditions, Maximum Power Point Tracking (MPPT) techniques are utilized. MPPT strategies can be classified into three categories [10]:

IJIREEICE ISSN (O) 2321-2004, ISSN (P) 2321-5526

International Journal of Innovative Research in Electrical, Electronics, Instrumentation and Control Engineering

Impact Factor 8.414 ⁜ Peer-reviewed & Refereed journal ⁜ Vol. 13, Issue 11, November 2025

DOI: 10.17148/IJIREEICE.2025.131119

WT Parameter-Based Methods:
These methods necessitate an understanding of the characteristics of the wind turbine.
Examples include the Tip Speed Ratio (TSR) and Optimal Torque Control (OTC) methods [11, 12, 13].
Sensorless Methods:
These methods do not require the estimation of wind speed or knowledge of turbine characteristics.
An example is the Perturb and Observe (P&O) algorithm [14].

C. Advancements in MPPT Techniques

To address the limitations of Perturb and Observe (P&O), researchers have investigated hybrid and intelligent control strategies:
Modified P&O (MPO): This method combines with other techniques such as Power Signal Feedback (PSF) [24], Optimal Relation-Based (ORB) MPPT [25], and adaptive step-size methods [26, 27, 28].
Fuzzy Logic Control (FLC): This approach improves MPPT by making real-time adjustments based on variations in input [31, 32, 33, 34, 35, 36].
Artificial Neural Networks (ANN) and Metaheuristic Optimization: These are utilized in MPPT techniques but tend to involve greater computational complexity and higher implementation costs [38, 39, 40].

D. Proposed Hybrid MPPT Approach

In order to overcome the shortcomings of conventional Perturb and Observe (P&O) methods and enhance Maximum Power Point Tracking (MPPT) efficiency, this research combines Fuzzy Logic Control (FLC) with the Trapezoidal Rule. The suggested approach functions in the following manner:
Trapezoidal Rule: Retrieves the maximum power and voltage values from the rectified current and voltage.
FLC Implementation: Establishes the duty cycle for more effectively tracking the Maximum Power Point (MPP) compared to traditional P&O methods.

II. CONNECTED IDEAS

Figure 1 illustrates the block diagram representation of the wind power system. In accordance with the Betz limit, the wind turbine (WT) is capable of capturing only 59% of the energy available in the wind, as depicted in Figure 1. Equation (1) defines Pm, the mechanical power extracted from the WT. Expression (2) describes the pair, or the power contained within the air, where ρ represents the air density, V denotes the wind velocity in meters per second (m/s), and A signifies the swept area covered by the turbine blades, measured in square meters (m2).

Expression 3 defines the radius as R. Cp represents the power coefficient, while the angular velocity is denoted in radians per second as ω, and the tip speed ratio is represented as λ.

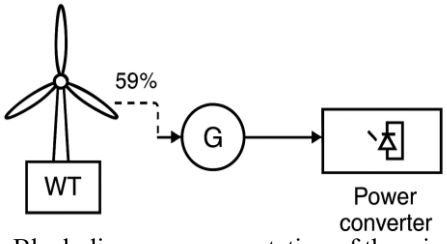

FIGURE 1: Block diagram representation of the wind power system

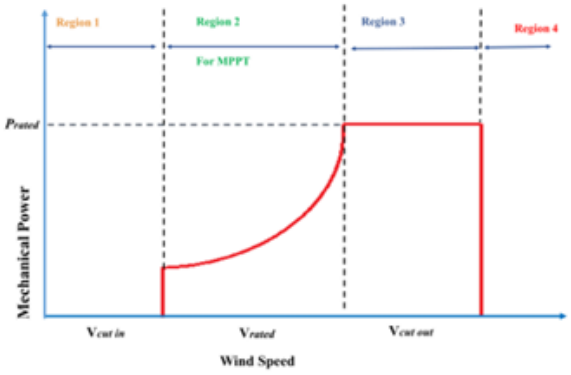

FIGURE 2. WECS operating regions [44].

IJIREEICE ISSN (O) 2321-2004, ISSN (P) 2321-5526

International Journal of Innovative Research in Electrical, Electronics, Instrumentation and Control Engineering

Impact Factor 8.414 ⁜ Peer-reviewed & Refereed journal ⁜ Vol. 13, Issue 11, November 2025

DOI: 10.17148/IJIREEICE.2025.131119

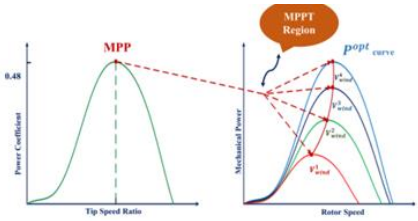

FIGURE 3. WT characteristics for λ opt and Cpopt . [44].

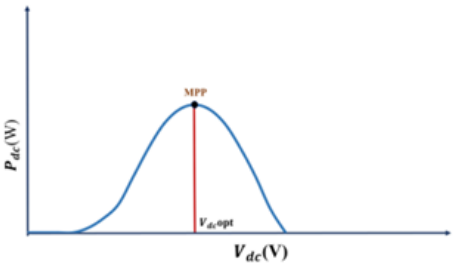

FIGURE 4. Relation between Vdc and Pdc.

The pair signifies the power contained within the wind and the power that is absorbed, with the value indicated in expression (4) being constrained to below 59% by the wind turbine WTis. Equations 1, 2, 3, and 4 are referenced in [26]. The generator stage receives input from the WT, facilitating the conversion of mechanical energy into electrical energy. The three-phase rectifier processes the generator's three-phase output to convert it to DC. The MPPT algorithm oversees the DC-DC boost conversion, which is enabled by the boost converter stage. The pulse width modulation (PWM) generator takes the duty cycle generated by the employed algorithm and utilizes it to control the switching element, thereby increasing the voltage and, as a result, the power. The various output power zones of the WECS are illustrated in Figure 2. The initial area depicts the condition where the WT cannot produce any electricity due to the wind's very low speed. The control element for maximizing power from the WECS is particularly important in the region between the cut-in and rated wind speeds. In the third region, the wind speed is between the rated and cutout levels, ensuring system protection. The fourth and final region represents wind speeds that exceed the cutout values.

$$P_m = \frac{1}{2}\rho A V^3 C_p(\lambda, \beta) \quad (1)$$

$$pair = \frac{1}{2}\rho A V^3 \quad (2)$$

$$\lambda = \frac{R*\omega}{V} \quad (3)$$

$$C_p = \frac{P_{windturbine}}{pair} \quad (4)$$

The second operational area, in which the MPPT method is employed to maximize power extraction from WECS, serves as the main emphasis of this study. The concept of MPPT for WECS is effectively illustrated in Figure 3. Maximum power extraction is achievable when the WECS functions along the optimal power curve. The MPPT algorithm facilitates the operation of the WECS at this curve. Consequently, the MPPT algorithm aids in recording and monitoring the peak output power for WECS.

A. Suggested MPPT Methods

Choosing the appropriate step is crucial for avoiding oscillations around the Maximum Power Point (MPP) and for achieving quicker tracking, as the Constant Power Output (CPO) technique determines the MPP by analyzing both past and present values of the rectified voltage. A trade-off seems to exist between these two aspects. The proposed method addresses this issue. The correlation between Vdc and Pdc [37] is illustrated in Figure 4, which also indicates the selection of step size for CPO. An optimal value of Vdc results in the maximum Pdc (MPP). This relationship forms the basis of the proposed method. The three phases in which the suggested approach functions are represented in Figure 6. In the initial phase, the Vdc-Pdc graph is divided into trapezoids of equal width using the trapezoidal rule. The second phase involves comparing the current and previous trapezoids to ascertain the values of maximum area and power. This concept is depicted in Figure 7. The data obtained are utilized to implement the Fuzzy Logic Controller (FLC) and to track the

IJIREEICE ISSN (O) 2321-2004, ISSN (P) 2321-5526

International Journal of Innovative Research in Electrical, Electronics, Instrumentation and Control Engineering

Impact Factor 8.414 ⁜ Peer-reviewed & Refereed journal ⁜ Vol. 13, Issue 11, November 2025

DOI: 10.17148/IJIREEICE.2025.131119

MPP in the third phase. Figure 8 presents the fundamental framework of the FLC. The values derived from applying the trapezoidal rule are Pout and Vout, which are also provided to the FLC. The input error, denoted as "e," and the change in error, represented as "ec," are calculated using the ratios of δP and δV, as outlined in Equations 5 and 6. The FLC inputs "e" and "ec" are defined by Equations 7, 8, and 9, respectively.

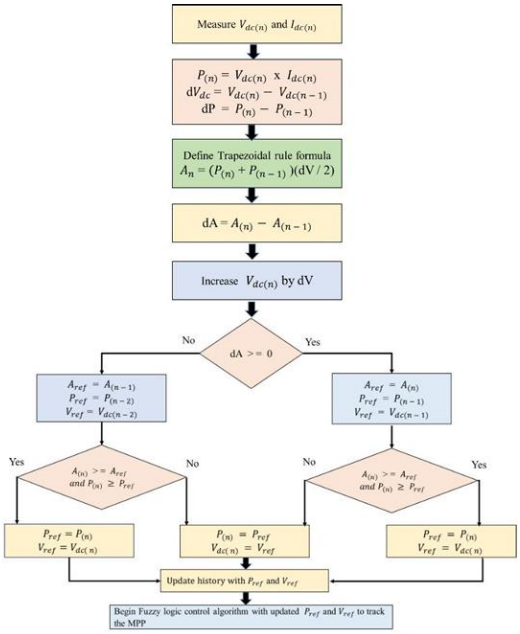

FIGURE 5. Procedure of the proposed MPPT method.

The defuzzification method employed is the centroid technique, while the type of Fuzzy Inference System (FIS) used is Mamdani. The implication and aggregation processes are characterized by minimum (min) and maximum (max), respectively. The FLC is capable of effectively tracking changes in wind speed. The inputs "e" and "ec," which are forwarded to the controller, are fuzzified to form the fuzzy set. To generate the appropriate fuzzy output, the inference system processes the fuzzy set using fuzzy rules. After defuzzification, the fuzzy output is ultimately converted into the duty cycle, which is then used to further control the switching element of the boost converter and facilitate MPP tracking.

$$\delta P = P_{(n)} - P_{(n-1)} \quad (5)$$

$$\delta V = V_{(n)} - V_{(n-1)} \quad (6)$$

$$e_{(n)} = \delta P / \delta V \quad (7)$$

$$ec = e_{(n)} - e_{(n-1)} \quad (8)$$

The membership function corresponding to the inputs "e," "ec," and "D" is illustrated in Figures 9, 10, and 11. These membership functions encompass seven defined variables: Nbig, Nmed, Nsmall, Zero, Psmall, Pmed, and Pbig. The complex reasoning behind the fuzzy rules is detailed as follows:

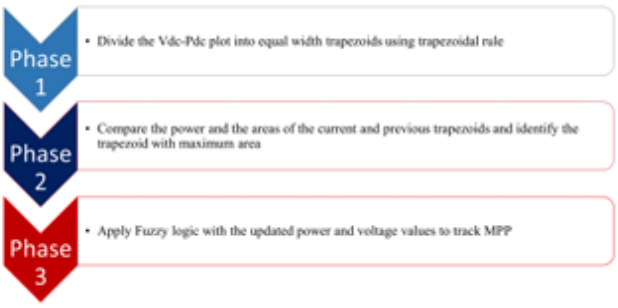

FIGURE 6. Phases of the proposed technique.

IJIREEICE ISSN (O) 2321-2004, ISSN (P) 2321-5526

International Journal of Innovative Research in Electrical, Electronics, Instrumentation and Control Engineering

Impact Factor 8.414 ⁜ Peer-reviewed & Refereed journal ⁜ Vol. 13, Issue 11, November 2025

DOI: 10.17148/IJIREEICE.2025.131119

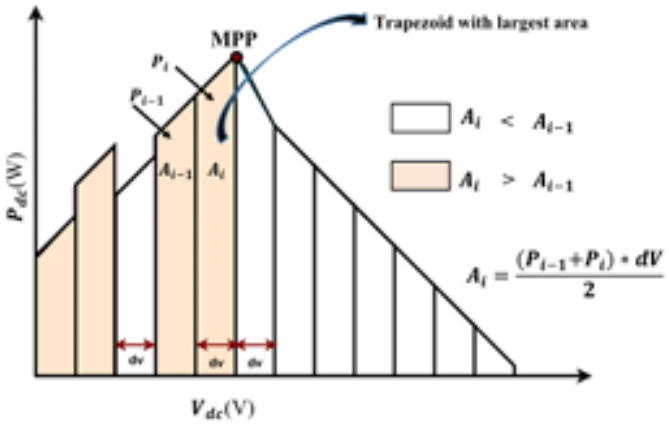

FIGURE 7. Theme of the proposed technique

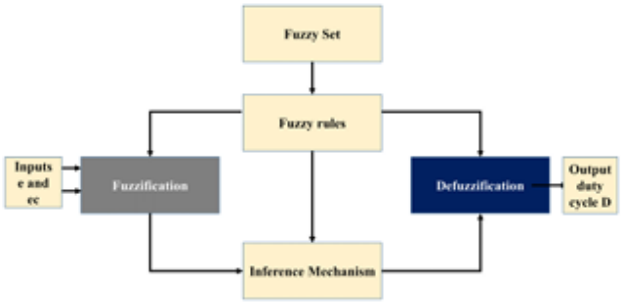

FIGURE 8. Basic frame work of FLC.

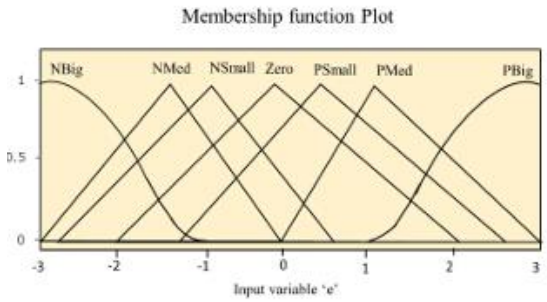

FIGURE 9. FLC input e membership function.

D = Zero if e = NBig and ec = NBig.
D=Zero if e = NBig and ec = NMed;
D = 0 if e = NBig and ec = NSmall.

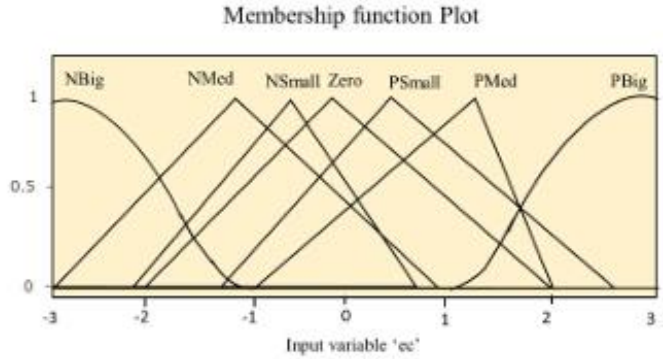

FIGURE 10. FLC input ec membership function.

IJIREEICE ISSN (O) 2321-2004, ISSN (P) 2321-5526

International Journal of Innovative Research in Electrical, Electronics, Instrumentation and Control Engineering

Impact Factor 8.414 ⁜ Peer-reviewed & Refereed journal ⁜ Vol. 13, Issue 11, November 2025

DOI: 10.17148/IJIREEICE.2025.131119

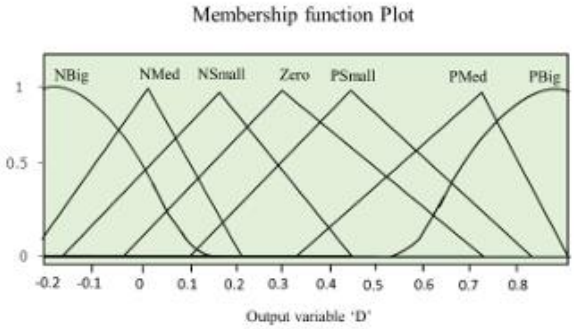

FIGURE 11. FLC output D membership function.

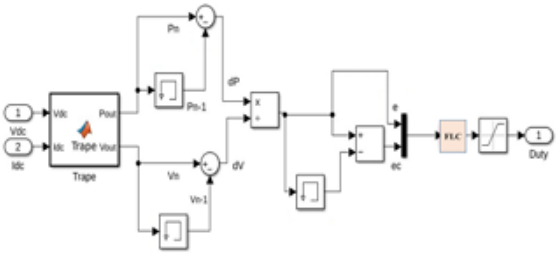

FIGURE 12. Fuzzy logic applied after trapezoidal rule in the proposed algorithm.

III. CPO SIMULATION AND THE SUGGESTED METHODS

The WECS model incorporating the TRPO, CPO, and the proposed trapezoidal rule-based FLC MPPT methods is illustrated in Figure 13 and is executed using MATLAB/Simulink. The WECS operates by simulating one method at a time through a manual switch. The parameters of the simulated system are presented in Table 3. The Simulink CPO block is depicted in Figure 14. The Simulink model for the TRPO method is shown in Figure 15, while the blocks for this technique are represented in Figure 16.

TABLE 2. Rules for FLC.

Output D	Input 'e'							
Input 'ec'		NBig	NMed	NSmall	Zero	PSmall	PMed	PBig
	NBig	Zero	Zero	NSmall	NMed	PSmall	PMed	PBig
	NMed	Zero	Zero	Zero	NSmall	PMed	PMed	PBig
	NSmall	Zero	Zero	Zero	Zero	PMed	PMed	PBig
	Zero	NBig	NSmall	Zero	Zero	PSmall	Zero	Zero
	PSmall	NBig	NMed	NSmall	Zero	Zero	Zero	Zero
	NMed	NBig	NMed	NSmall	PSmall	Zero	Zero	Zero
	PBig	NMed	NMed	NSmall	PMed	Zero	Zero	Zero

TABLE 3. Simulation system parameters.

WT Parameters	Value and unit
Radius	3.01m
Air density	$1.22 kg/m^3$
Rated Power	1 Kilo Watt
β	0
PMSG Parameters	**Value and unit**
Rated Power	1 Kilo Watt
Pole pairs	2
Rs	1.6 Ω
Ld=Lq	6.3 miliHenry
J	$8.54\ kgm^2$
Boost converter Parameters	**Value and unit**
L	75 miliHenry
C	0.468 μFarads
Switching frequency	5KHz
RL	54 Ω

The power coefficient for each of the three methods is illustrated in Figure 17.

IJIREEICE ISSN (O) 2321-2004, ISSN (P) 2321-5526

International Journal of Innovative Research in Electrical, Electronics, Instrumentation and Control Engineering

Impact Factor 8.414 ⁜ Peer-reviewed & Refereed journal ⁜ Vol. 13, Issue 11, November 2025

DOI: 10.17148/IJIREEICE.2025.131119

The random variations in wind speed used to simulate all three methods are depicted in Figure 18. The curve for the proposed technique is represented in red, TRPO's in light blue, and the CPO method's in navy blue. The relative voltage, current, and DC output power achieved with each of the three methods are presented in Figures 19, 20, and 21 respectively. The markings A, B, C, D, and E in these figures indicate the enhanced output power, voltage, and current, along with the reduction in oscillations. These figures clearly demonstrate that the proposed method contributes to reducing oscillations and enhancing the output power produced.

IV. OUTCOMES

The TRPO, CPO, and the proposed MATLAB/Simulink method have all been simulated in the previous section. The power coefficient for each of the three techniques is depicted in Figure 17. Table 3 details the specifications of the simulated system. Figure 18 demonstrates the variations in wind speed. The graphs displayed in Figures 19, 20, and 21 respectively indicate higher generated voltage, current, and power.

TABLE 4. Comparison of the rise time. response time and the transient time of all the three simulated techniques.

Name of the MPPT algorithm	Rise time (m sec)	Transient time (m sec)	Response time (m sec)
Trapezoidal rule based Fuzzy logic	0.1231	6.9450	0.035
Trapezoidal rule based PO	0.2133	6.9450	0.040
Conventional P&O	0.3200	6.9700	0.060

TABLE 5. Comparison of the tracking efficiency for all the three techniques at the rated wind speed of 5 m/s.

Name of the MPPT algorithm	MPPTracking efficiency
Trapezoidal rule based Fuzzy logic	99.1%
Trapezoidal rule based P&O	92.7%
Conventional P&O	87%

The effectiveness of the proposed algorithm is illustrated through the methodology employed alongside the other two. Sections A, B, C, and D of these figures indicate an increase in output power and a reduction in oscillations. For each of the three methods, the wind speed was randomly varied among 4, 5, 4, 3, and 5 m/sec. The rated wind speed of 5 m/s produces the highest simulated power output across all methods. The recommended TRPO and CPO methods exhibit maximum duty cycles of 0.37, 0.302, and 0.29, respectively. Table 4 presents a comparison of the rise time, response time, and transient time for the three simulated methods. The implementation of the TRPO method results in a 0.6%, 6.8%, and 1.06% increase in voltage, current, and power at the output when compared to CPO, respectively. The comparison illustrated in Table 4 clearly indicates that the proposed method offers a quicker response in tracking the MPP. Table 5 reveals that the tracking efficiency of the proposed method while following the MPP is the highest among all three techniques; Table 6 further confirms the superiority of the proposed method.

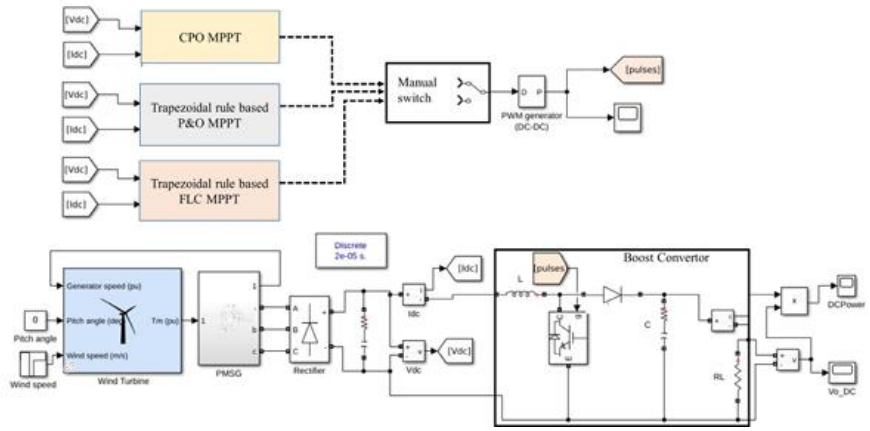

FIGURE 13. Simulation Model in MATLAB/Simulink for the TRPO, CPO and the proposed algorithm.

IJIREEICE ISSN (O) 2321-2004, ISSN (P) 2321-5526

International Journal of Innovative Research in Electrical, Electronics, Instrumentation and Control Engineering

Impact Factor 8.414 ⁜ Peer-reviewed & Refereed journal ⁜ Vol. 13, Issue 11, November 2025

DOI: 10.17148/IJIREEICE.2025.131119

TABLE 6. Comparison of the MPPT techniques.

Parameters of the MPPT technique	TSR [15], [45]–[48]	PSF [15], [45], [46]	OT [15], [45]–[48]	CPO [15], [45]–[48]	INC [15], [45]–[48]	ORB [15], [45]–[48]	NN [45], [47]	TRPO [43]	Proposed Technique
Efficiency of Tracking MPP	High	Moderate	Moderate	Low	Low	Moderate	High	High	High
Convergence speed	High	High	High	Low	Low	Medium	High	High	High
Oscillations near the MPP	No	No	No	Yes	Yes	No	No	No	No
Training data requirement	No	Yes	Yes	No	No	No	Yes	No	No
Wind speed estimation sensor requirement	Yes	Yes	No	No	No	No	Depends	No	No
Performance under changing wind speed	High	Moderate	High	Moderate	Moderate	Moderate	High	High	Excellent

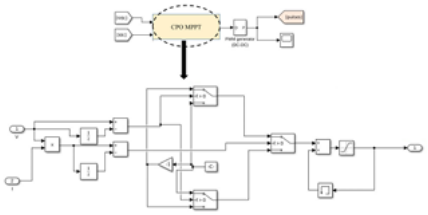

FIGURE 14. CPO technique SIMULINK block.

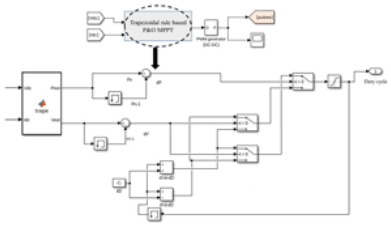

FIGURE 15. SIMULINK block for TRPO algorithm.

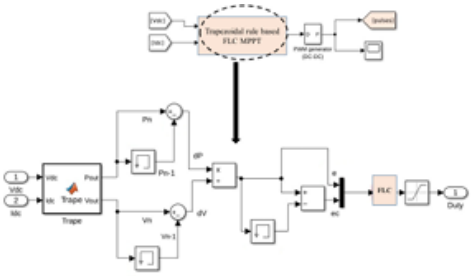

FIGURE 16. Simulation block for the presented technique in MATLAB/Simulink.

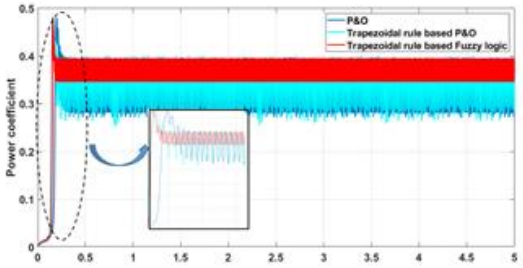

FIGURE 17. Plot of the Power coefficient

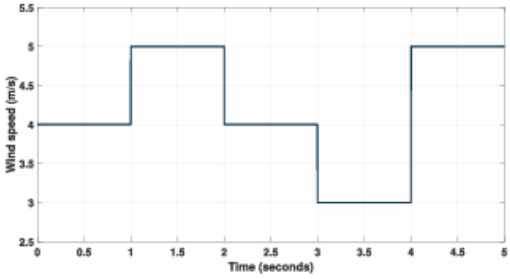

FIGURE 18. Profile of variation in the wind speed.

IJIREEICE ISSN (O) 2321-2004, ISSN (P) 2321-5526

International Journal of Innovative Research in Electrical, Electronics, Instrumentation and Control Engineering

Impact Factor 8.414 ⁜ Peer-reviewed & Refereed journal ⁜ Vol. 13, Issue 11, November 2025

DOI: 10.17148/IJIREEICE.2025.131119

V. DISCUSSION

Numerous MPPT methods for Wind Energy Conversion Systems (WECS) are documented in the literature, and it is noted that enhancing one performance parameter in the existing methods designed for Maximum Power Point (MPP) tracking can lead to a decline in another. The primary challenge lies in optimizing system performance under highly variable wind conditions while maximizing power output through the MPPT technique, all while minimizing computational demands and oscillations around the MPP. Although MPPT-based optimization techniques are well-established, they often encounter challenges such as increased computational load during MPP tracking. The latest hybrid methods available can address the shortcomings of traditional techniques; however, they tend to be complex in their implementation, highlighting the need for simpler approaches to achieve this goal.

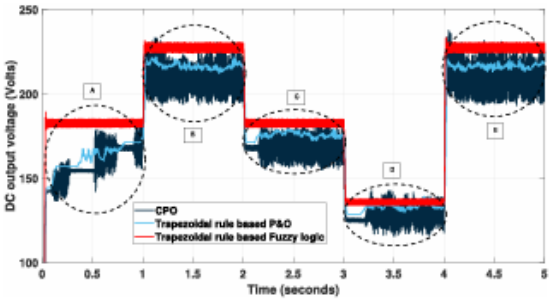

FIGURE 19. Plot of Time and output Voltage.

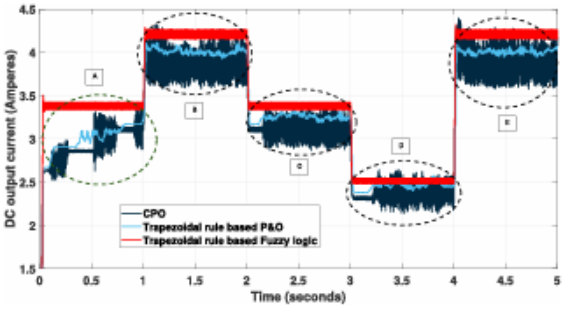

FIGURE 20. Plot of Time and output Current.

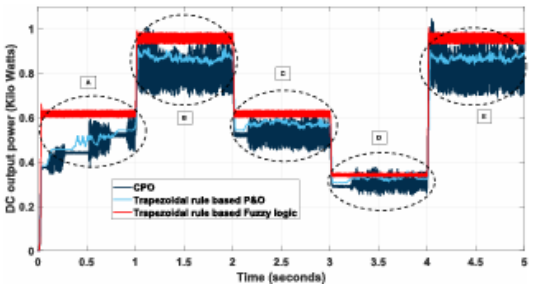

FIGURE 21. Plot of Time and output Power.

ANN Architecture

- "In the hybrid system for MPPT, we implemented a feedforward neural network (FFNN), which is an excellent option for managing the non-linearities associated with wind and solar energy.
- The FFNN consists of an input layer (including wind speed 'Vw' (m/s), solar irradiance 'G' (W/m²), PV voltage 'Vpv' (V), and PV current 'Ipv' (A)), two hidden layers (each containing 10 neurons with ReLU activation), and an output layer (duty cycles 'd_wind' and 'd_solar' within a range of 0 to 1).
- ReLU is effective and helps to prevent the issue of vanishing gradients.

ANN Training Process

- "The ANN was trained using 10,000 samples sourced from MATLAB/Simulink (Vw: 0-25 m/s, with increments of 0.1 m/s; G: 0-1000 W/m², with increments of 10 W/m²).

IJIREEICE ISSN (O) 2321-2004, ISSN (P) 2321-5526

International Journal of Innovative Research in Electrical, Electronics, Instrumentation and Control Engineering

Impact Factor 8.414 ⁜ Peer-reviewed & Refereed journal ⁜ Vol. 13, Issue 11, November 2025

DOI: 10.17148/IJIREEICE.2025.131119

- The Adam optimizer was employed (learning rate: 0.001, beta1: 0.9, beta2: 0.999, epsilon: 1e-7) utilizing mini-batches of 32 samples.
- Mean Squared Error (MSE) served as the loss function, and 10-fold cross-validation was implemented to mitigate overfitting.
- Inputs were normalized to a range of 0-1 through min-max scaling to enhance the training process.

ANN Inputs and Outputs

- "The inputs for the ANN include: Vw (m/s), G (W/m²), Vpv (V), and Ipv (A).
- The outputs consist of duty cycles (ranging from 0 to 1): d_wind (for the wind converter) and d_solar (for the solar converter).
- These outputs are utilized to control DC-DC converters aimed at maximizing power extraction."

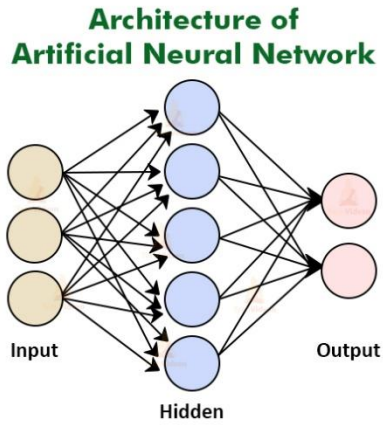

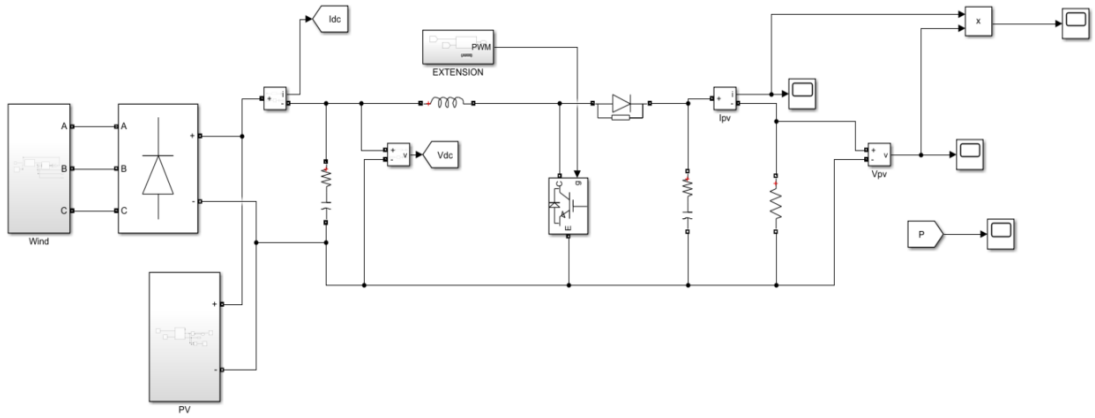

Figure 21: Block diagram of solar and wind with ANN

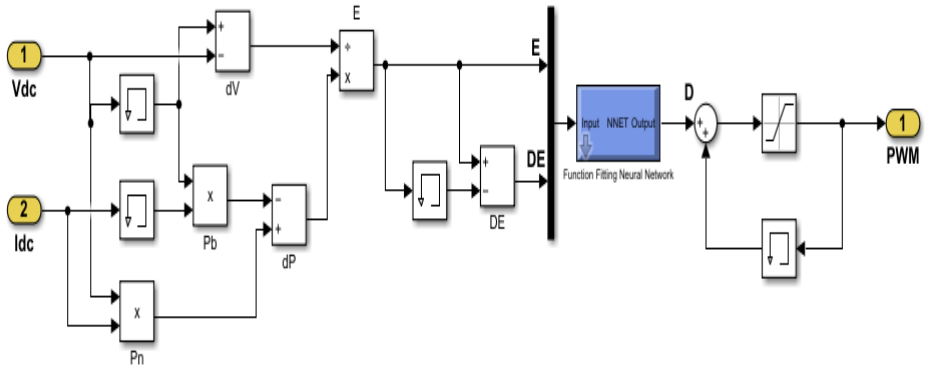

Figure 22: Simulation block for the ANN MPPT technique in MATLAB/Simulink.

IJIREEICE ISSN (O) 2321-2004, ISSN (P) 2321-5526

International Journal of Innovative Research in Electrical, Electronics, Instrumentation and Control Engineering

Impact Factor 8.414 ⁜ Peer-reviewed & Refereed journal ⁜ Vol. 13, Issue 11, November 2025

DOI: 10.17148/IJIREEICE.2025.131119

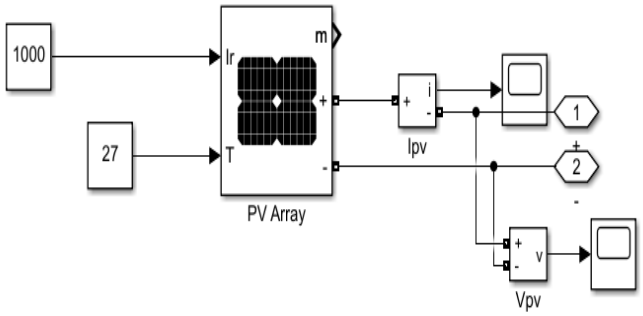

Figure 23: Simulation block for the PV in MATLAB/Simulink.

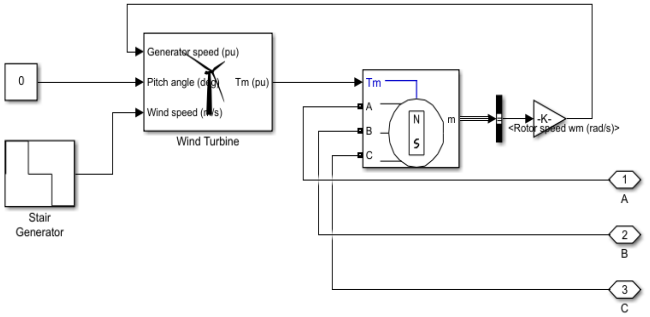

Figure 24: Simulation block for the Wind in MATLAB/Simulink.

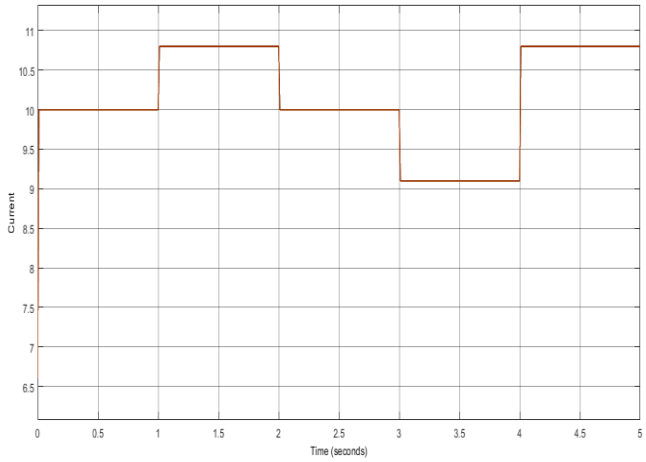

Figure 22: Plot of Time and output Current.

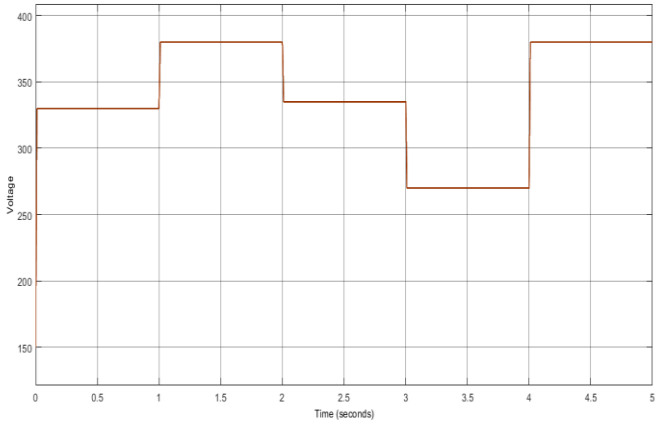

Figure 23: Plot of Time and output Voltage

IJIREEICE ISSN (O) 2321-2004, ISSN (P) 2321-5526
International Journal of Innovative Research in Electrical, Electronics, Instrumentation and Control Engineering
Impact Factor 8.414 ⁜ Peer-reviewed & Refereed journal ⁜ Vol. 13, Issue 11, November 2025
DOI: 10.17148/IJIREEICE.2025.131119

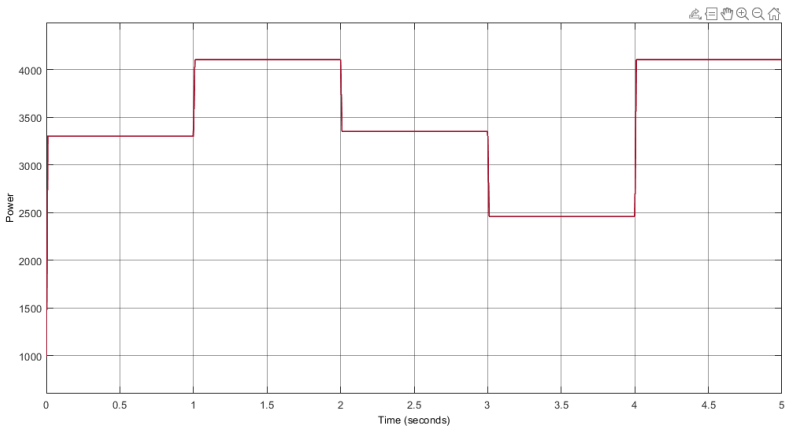

Figure 24: Plot of Time and output Power

Integration of Wind-Solar Hybrid System with ANN

To improve the efficiency of power generation, a hybrid wind-solar energy system is proposed, wherein both renewable sources contribute to the overall energy output. The integration of an Artificial Neural Network (ANN) enhances Maximum Power Point Tracking (MPPT) by adapting to varying environmental conditions and optimizing power extraction. In the subsequent sections, we will examine the implementation of the suggested method utilizing numerical techniques and intelligent control algorithms to maximize power efficiency.

The power present in the wind (Pair) and the power captured by the Wind Turbine (WT) are associated with the Betz limit, which states that no more than 59% of the wind's energy can be captured by the turbine. This constraint is a fundamental aspect of wind energy conversion. The pertinent equations for mechanical power extraction and wind power, along with the turbine's swept area and radius, are specified in Equations (1), (2), (3), and (4), which can be referenced in [26].

Mechanical Energy Conversion

The generator stage receives input from the wind turbine, enabling the transformation of mechanical energy into electrical energy. A three-phase rectifier converts the generator's three-phase output into direct current (DC). The Maximum Power Point Tracking (MPPT) algorithm manages the DC-DC boost converter, which elevates the DC voltage. This operation is regulated through a Pulse Width Modulation (PWM) generator, which receives the duty cycle generated by the MPPT algorithm. By modifying the duty cycle, the PWM governs the switching element in the boost converter, thereby increasing the output voltage and, as a result, the total power.

Wind Turbine Output Power Zones

The wind turbine functions across various output power zones. These zones are characterized as follows:

• Zone 1: This area signifies wind speeds that are insufficient for the wind turbine to produce any power.

• Zone 2: Spanning from the cut-in to the rated wind speeds, the turbine begins to generate power, and this range is essential for optimizing efficiency via MPPT.

• Zone 3: In this area, as wind speeds surpass the rated wind speed, the power output of the turbine starts to stabilize.

Integration of Wind and Solar Energy with ANN

To enhance energy generation, a hybrid wind-solar energy system is utilized. This system merges the advantages of both renewable sources to fulfill energy requirements more efficiently. An Artificial Neural Network (ANN) is implemented to enhance the performance of the Maximum Power Point Tracking (MPPT) algorithm, enabling the system to adjust dynamically to fluctuating wind and solar conditions. The ANN aids in predicting the maximum power point with greater efficiency, modifying the duty cycle for both wind and solar power inputs.

• Wind Energy System (WECS): The wind energy conversion system harnesses energy from the wind via a wind turbine and generator.

• Solar Energy System (PV): The solar power system employs photovoltaic (PV) panels to produce electricity from sunlight.

• ANN Extension: The ANN model is incorporated to optimize MPPT for both wind and solar inputs, improving the system's efficiency and minimizing energy losses due to environmental variations.

By integrating these systems and employing sophisticated control algorithms, the hybrid system maximizes energy capture and stability, delivering a dependable and efficient renewable energy solution.

DOI: 10.17148/IJIREEICE.2025.131119

Choosing the correct step size is vital to prevent oscillations around the Maximum Power Point (MPP) and to ensure rapid tracking. The Conventional Perturb and Observe (CPO) algorithm accomplishes MPP tracking by evaluating past and current rectified voltage values, which creates a trade-off between stability and tracking speed. The proposed method effectively resolves this challenge.

Relationship Between VdcV_{dc}Vdc and PdcP_{dc}Pdc

The correlation between DC voltage (VdcV_{dc}Vdc) and DC power (PdcP_{dc}Pdc) is crucial for determining the step size in CPO. The Maximum Power Point (MPP) is attained when PdcP_{dc}Pdc is optimized for a suitable VdcV_{dc}Vdc value. This proposed method leverages this relationship to ensure effective tracking with minimal power loss.

Three-Stage Operation of the Proposed Method

The suggested MPPT algorithm functions through three primary stages

1. Trapezoidal Rule-Based Voltage Partitioning

The Vdc-Pdc graph is segmented into equal-width trapezoidal sections utilizing the trapezoidal numerical integration technique. This method guarantees precise power estimation across various voltage levels.

Comparison of Current and Previous Trapezoidal Areas

The areas beneath the trapezoidal segments are evaluated between successive iterations. The maximum power region and reference voltage are identified dynamically.

Fuzzy Logic Control (FLC) for Maximum Power Point (MPP) Tracking

The trapezoidal rule yields output power (PoutP_{out}Pout) and output voltage (VoutV_{out}Vout), which are utilized as inputs for the FLC.

The input error (e) and the change in error (ec) are determined based on perturbation values δP\delta PδP and δV\delta VδV, as outlined in Equations (5) and (6).

The fuzzy logic input equations are detailed in Equations (7), (8), and (9).

Fuzzy Inference System (FIS) Design

The FLC system incorporates:

- Mamdani-type Fuzzy Inference System (FIS)
- Defuzzification through the Centroid method
- Minimum (min) for implication and Maximum (max) for aggregation

Hybrid Wind-Solar System with ANN-Based MPPT

To enhance power tracking further, the proposed MPPT technique is integrated with a hybrid wind-solar energy system, utilizing an Artificial Neural Network (ANN) for improved decision-making:

• Wind Energy Conversion System (WECS): This system converts wind energy into electricity through the use of wind turbines, generators, and power converters.

• Solar Photovoltaic (PV) System: This system transforms sunlight into electricity, thereby complementing the generation of wind power.

• ANN Extension: The ANN is trained to adapt to various environmental conditions and offers dynamic adjustments to MPPT, thereby improving efficiency in response to changing wind and solar inputs.

This intelligent hybrid strategy overcomes the constraints of conventional methods, guaranteeing rapid, stable, and highly efficient MPPT tracking in diverse environmental conditions.

TABLE 7. Comparison of the MPPT techniques.

S.No	Parameters	Base Paper Output Result			Project Output Result
		CPO	TRPO	TRFL	ANN
1	Voltage In DC (Vdc)	130 V	150 V	180 V	340 V
2	Current In DC (Idc)	2.6 Amps	2.8 Amps	3.5 Amps	10 Amps
3	Power In DC (Pdc)	0.38 kw	0.4 kw	0.65 kw	3.4 kw

DOI: 10.17148/IJIREEICE.2025.131119

CPO	Conventional Perturb And Observe
TRPO	Trapezoidal Rule Based PO
TRFL	Trapezoidal Rule Based Fuzzy logic
ANN	Aritifical Neural Network

VI. CONCLUSION

The present condition of MPPT (Maximum Power Point Tracking) algorithms for Wind Energy Conversion Systems (WECS) showcases a diverse array of tracking strategies, ranging from conventional methods to sophisticated soft computing techniques and optimization-centric approaches. Although these contemporary methods have demonstrated effectiveness in precisely tracking the MPP, they frequently encounter heightened implementation complexity, rendering them less feasible for real-time or cost-effective applications. Consequently, there exists a significant demand for more straightforward and efficient tracking techniques. Previous studies have investigated the integration of traditional strategies, such as the Constant Power Output (CPO) method, with numerical techniques like the trapezoidal rule. Building upon this foundation, the method proposed in this study presents a hybrid approach that combines a trapezoidal rule-based technique with Fuzzy Logic Control (FLC), further augmented by an Artificial Neural Network (ANN). This three-phase method initiates by segmenting the Vdc-Pdc curve into equal-width trapezoids utilizing the trapezoidal rule. In the subsequent phase, the trapezoid associated with the maximum power output is determined. The concluding phase employs FLC to track the MPP within that trapezoid using the identified power and voltage values, while the ANN adaptively learns from the system's behavior to enhance tracking precision and responsiveness under fluctuating wind conditions. This methodology eliminates the necessity for a wind speed sensor and improves the robustness and efficiency of the tracking process. A comparative analysis with CPO and the Trapezoidal Rule-based Power Optimization (TRPO) methods under randomly fluctuating wind speeds (4, 5, 4, 3, and 5 m/s) indicates that while all methods attain peak power at a rated wind speed of 5 m/s, the proposed technique significantly surpasses the others. Specifically, the TRPO method yields 0.6%, 6.8%, and 1% superior output in terms of voltage, current, and power, respectively, when compared to CPO. The suggested trapezoidal rule-based FLC with ANN produces 5.4%, 5.4%, and 7.36% greater output.

REFERENCES

[1]. A. K. Aliyu, B. Modu, and C. W. Tan, "A review of renewable energy development in Africa: A focus in South Africa, Egypt and Nigeria," Renew. Sustain. Energy Rev., vol. 81, pp. 2502–2518, Jan. 2018.

[2]. A. Rajaei, M. Mohamadian, and A. Y. Varjani, "Vienna-rectifier based direct torque control of PMSG for wind energy applica tion," IEEE Trans. Ind. Electron., vol. 60, no. 7, pp. 2919–2929, Jul. 2013.

[3]. M. Singh and A. Chandra, "Application of adaptive network-based fuzzy inference system for sensorless control of PMSG-based wind turbine with nonlinear-load-compensation capabilities," IEEE Trans. Power Electron., vol. 26, no. 1, pp. 165–175, Jan. 2011.

[4]. Z. Chen, J. M. Guerrero, and F. Blaabjerg, "A review of the state of the art of power electronics for wind turbines," IEEE Trans. Power Electron., vol. 24, no. 8, pp. 1859–1875, Aug. 2009.

[5]. H. Li and Z. Chen, "Overview of different wind generator systems and their comparisons," IET Renew. Power Gener., vol. 2, no. 2, pp. 123–138, Jun. 2008.

[6]. Z. Alnasir and M. Kazerani, "An analytical literature review of stand-alone wind energy conversion systems from generator viewpoint," Renew. Sustain. Energy Rev., vol. 28, pp. 597–615, Dec. 2013.

[7]. M. J. Duran, F. Barrero, A. Pozo-Ruz, F. Guzman, J. Fernandez, and H. Guzman, "Understanding power electronics and electrical machines in multidisciplinary wind energy conversion system courses," IEEE Trans. Educ., vol. 56, no. 2, pp. 174–182, May 2013.

[8]. M. Cheng and Y. Zhu, "The state of the art of wind energy conversion systems and technologies: A review," Energy Convers. Manage., vol. 88, pp. 332–347, Dec. 2014.

[9]. A. Mirecki, X. Roboam, and F. Richardeau, "Architecture complexity and energy efficiency of small wind turbines," IEEE Trans. Ind. Electron., vol. 54, no. 1, pp. 660–670, Feb. 2007.

[10]. S. Lalouni, D. Rekioua, K. Idjdarene, and A. Tounzi, "Maximum power point tracking based hybrid hill-climb search method applied to wind energy conversion system," Electr. Power Compon. Syst., vol. 43, nos. 8–10, pp. 1028–1038, Jun. 2015.

[11]. A. Dahbi, M. Hachemi, N. Nait-Said, and M.-S. Nait-Said, "Realization and control of a wind turbine connected to the grid by using PMSG," Energy Convers. Manage., vol. 84, pp. 346–353, Aug. 2014.

[12]. C.-M. Hong, C.-H. Chen, and C.-S. Tu, "Maximum power point tracking-based control algorithm for PMSG wind generation system with out mechanical sensors," Energy Convers. Manage., vol. 69, pp. 58–67, May 2013.

DOI: 10.17148/IJIREEICE.2025.131119

[13]. J. S. Thongam, P. Bouchard, R. Beguenane, A. F. Okou, and A. Merabet, "Control of variable speed wind energy conversion system using a wind speed sensorless optimum speed MPPT control method," in Proc. 37th Annu. Conf. IEEE Ind. Electron. Soc. (IECON), Nov. 2011, pp. 855–860.

[14]. O. Carranza, E. Figueres, G. Garcerá, R. Ortega, and D. Velasco, "Low power wind generation system based on variable speed permanent magnet synchronous generators," in Proc. IEEE Int. Symp. Ind. Electron., Jun. 2011, pp. 1063–1068.

[15]. M. A. Abdullah, A. H. M. Yatim, C. W. Tan, and R. Saidur, "A review of maximum power point tracking algorithms for wind energy sys tems," Renew. Sustain. Energy Rev., vol. 16, no. 5, pp. 3220–3227, Jun. 2012.

[16]. Q. Mei, M. Shan, L. Liu, and J. M. Guerrero, "A novel improved variable step-size incremental-resistance MPPT method for PV sys tems," IEEE Trans. Ind. Electron., vol. 58, no. 6, pp. 2427–2434, Jun. 2011.

[17]. B. Lahfaoui, S. Zouggar, B. Mohammed, and M. L. Elhafyani, "Real time study of P&O MPPT control for small wind PMSG turbine systems using Arduino microcontroller," Energy Procedia, vol. 111, pp. 1000–1009, Mar. 2017.

[18]. A. Urtasun, P. Sanchis, I. S. Martín, J. López, and L. Marroyo, "Modeling of small wind turbines based on PMSG with diode bridge for sensorless maximum power tracking," Renew. Energy, vol. 55, pp. 138–149, Jul. 2013.

[19]. Y.Xia,K.H.Ahmed,andB.W.Williams,"Windturbinepowercoefficient analysis of a new maximum power point tracking technique," IEEE Trans. Ind. Electron., vol. 60, no. 3, pp. 1122–1132, Mar. 2013.

[20]. Z. M. Dalala, Z. U. Zahid, W. Yu, Y. Cho, and J.-S. Lai, "Design and analysis of an MPPT technique for small-scale wind energy conversion systems," IEEE Trans. Energy Convers., vol. 28, no. 3, pp. 756–767, Sep. 2013.

[21]. Y. Daili, J.-P. Gaubert, and L. Rahmani, "Implementation of a new maximum power point tracking control strategy for small wind energy con version systems without mechanical sensors," Energy Convers. Manage., vol. 97, pp. 298–306, Jun. 2015.

[22]. R.M.LinusandP. Damodharan,"Maximum power point tracking method using a modified perturb and observe algorithm for grid connected wind energy conversion systems," IET Renew. Power Gener., vol. 9, no. 6, pp. 682–689, Aug. 2015.

[23]. J. Pande, P. Nasikkar, K. Kotecha, and V. Varadarajan, "A review of maximum power point tracking algorithms for wind energy conversion systems," J. Mar. Sci. Eng., vol. 9, no. 11, p. 1187, Oct. 2021.

[24]. J.Chen,T.Lin,C.Wen, and Y. Song, "Design of a unified power controller for variable-speed fixed-pitch wind energy conversion system," IEEE Trans. Ind. Electron., vol. 63, no. 8, pp. 4899–4908, Aug. 2016.

[25]. S. Ahmed, M. A. Rashid, S. B. Mohamed, and S. B. Yaakob, "A novel maximum power point tracking algorithm for wind energy conversion system," Eng. Lett., vol. 27, no. 4, pp. 822–830, 2019.

[26]. H. H. H. Mousa, A. Youssef, and E. E. M. Mohamed, "Study of robust adaptive step-sizes P&O MPPT algorithm for high-inertia WT with direct driven multiphase PMSG," Int. Trans. Electr. Energy Syst., vol. 29, no. 10, pp. 1–18, Oct. 2019.

[27]. A.-R. Youssef, H. H. H. Mousa, and E. E. M. Mohamed, "Development of self-adaptive P&O MPPT algorithm for wind generation systems with concentrated search area," Renew. Energy, vol. 154, pp. 875–893, Jul. 2020.

[28]. S.-H. Mozafarpoor-Khoshrodi and G. Shahgholian, "Improvement of perturb and observe method for maximum power point tracking in wind energy conversion system using fuzzy controller," Energy Equip. Syst., vol. 4, no. 2, pp. 111–122, Dec. 2016.

[29]. H. H. H. Mousa, A.-R. Youssef, and E. E. M. Mohamed, "Modified P&O MPPTalgorithm for optimal power extraction of five-phase PMSG based wind generation system," Social Netw. Appl. Sci., vol. 1, no. 8, p. 838, Aug. 2019.

[30]. E. H. Abdou, A.-R. Youssef, S. Kamel, and M. M. Aly, "Sensor less proposed multi sector perturb and observe maximum power tracking for 1.5 MWbasedonDFIG,"J. Control Instrum. Eng., vol. 6, no. 1, pp. 1–13, 2020.

[31]. X.-X. Yin, Y.-G. Lin, W. Li, H.-W. Liu, and Y.-J. Gu, "Fuzzy logic sliding-mode control strategy for extracting maximum wind power," IEEE Trans. Energy Convers., vol. 30, no. 4, pp. 1267–1278, Dec. 2015.

[32]. M. Farbood, M. Shasadeghi, A. Izadian, and T. Niknam, "Fuzzy model predictive MPPT control of interconnected wind turbines drivetrain," Asian J. Control, vol. 24, no. 5, pp. 2714–2728, Sep. 2022.

[33]. A. A. Salem, N. A. N. Aldin, A. M. Azmy, and W. S. E. Abdellatif, "Implementation and validation of an adaptive fuzzy logic controller for MPPT of PMSG-based wind turbines," IEEE Access, vol. 9, pp. 165690–165707, 2021.

[34]. M. Zerouali, M. Boutouba, A. E. Ougli, and B. Tidhaf, "Control of variable speed wind energy conversion systems by fuzzy logic and conventional P&O," in Proc. Int. Conf. Intell. Syst. Adv. Comput. Sci. (ISACS), Dec. 2019, pp. 1–5.

[35]. R. Tiwari and N. R. Babu, "Fuzzy logic based MPPT for permanent magnet synchronous generator in wind energy conversion system," IFAC PapersOnLine, vol. 49, no. 1, pp. 462–467, 2016.

[36]. A. M. Eltamaly and H. M. Farh, "Maximum power extraction from wind energy system based on fuzzy logic control," Electr. Power Syst. Res., vol. 97, pp. 144–150, Apr. 2013.

DOI: 10.17148/IJIREEICE.2025.131119

[37]. K. Chaicharoenaudomrung, K. Areerak, K. Areerak, S. Bozhko, and C. I. Hill, "Maximum power point tracking for stand-alone wind energy conversion system using FLC-P&Omethod,"IEEJTrans.Electr.Electron. Eng., vol. 15, no. 12, pp. 1723–1733, Dec. 2020.

[38]. N. Priyadarshi, V. Ramachandaramurthy, S. Padmanaban, and F. Azam, "An ant colony optimized MPPT for standalone hybrid PV-wind power system with single cuk converter," Energies, vol. 12, no. 1, p. 167, Jan. 2019.

[39]. C. Sompracha, D. Jayaweera, and P. Tricoli, "Particle swarm optimi sation technique to improve energy efficiency of doubly-fed induction generators for wind turbines," J. Eng., vol. 2019, no. 18, pp. 4890–4895, Jul. 2019.

[40]. B. Yang, X. Zhang, T. Yu, H. Shu, and Z. Fang, "Grouped grey wolf optimizer for maximum power point tracking of doubly-fed induction generator based wind turbine," Energy Convers. Manage., vol. 133, pp. 427–443, Feb. 2017.

[41]. N. M. M. Altwallbah, M. A. M. Radzi, N. Azis, S. Shafie, and M. A. A. M. Zainuri, "New perturb and observe algorithm based on trapezoidal rule: Uniformandpartialshadingconditions,"EnergyConvers. Manage., vol. 264, Jul. 2022, Art. no. 115738.

[42]. S. Heier, *Grid Integration of Wind Energy Conversion Systems*, 2nd ed. Chichester, U.K.: Wiley, 2014.

[43]. T. R. Ayodele, A. S. S. Sambo, and A. S. Aliyu, "Artificial Neural Network Based MPPT for Wind Energy Conversion System," *Energy Reports*, vol. 7, pp. 2101–2112, 2021.

[44]. K. Prakash and S. Sivanagaraju, "ANN Based MPPT Control of WECS under Varying Wind Speed Conditions," *Int. J. Renewable Energy Research (IJRER)*, vol. 3, no. 2, pp. 362–366, 2013.

[45]. S. J. Huang and F. S. Pai, "Design and operation of a fuzzy logic-based self-tuning maximum power point tracking controller for wind energy conversion systems," *IEEE Trans. Energy Convers.*, vol. 23, no. 2, pp. 632–640, Jun. 2008.

[46]. M. R. Patel, *Wind and Solar Power Systems: Design, Analysis, and Operation*, 2nd ed. Boca Raton, FL, USA: CRC Press, 2005.